HAL
open science

Degradation of γ-irradiated polyethylene-ethylene vinyl alcohol-polyethylene multilayer films: An ESR study

Gérard Audran, Samuel Dorey, Nathalie Dupuy, Fanny Gaston, Sylvain R.A. Marque

To cite this version:

Gérard Audran, Samuel Dorey, Nathalie Dupuy, Fanny Gaston, Sylvain R.A. Marque. Degradation of γ-irradiated polyethylene-ethylene vinyl alcohol-polyethylene multilayer films: An ESR study. Polymer Degradation and Stability, 2015, 122, pp.169 - 179. 10.1016/j.polymdegradstab.2015.10.021 . hal-01451409

HAL Id: hal-01451409

https://hal.science/hal-01451409v1

Submitted on 12 Apr 2018

HAL is a multi-disciplinary open access archive for the deposit and dissemination of scientific research documents, whether they are published or not. The documents may come from teaching and research institutions in France or abroad, or from public or private research centers.

L'archive ouverte pluridisciplinaire **HAL**, est destinée au dépôt et à la diffusion de documents scientifiques de niveau recherche, publiés ou non, émanant des établissements d'enseignement et de recherche français ou étrangers, des laboratoires publics ou privés.

Degradation of γ-irradiated polyethylene-ethylene vinyl alcohol-polyethylene multilayer films: An ESR study

Gérard Audran [a], Samuel Dorey [b], Nathalie Dupuy [c], Fanny Gaston [a, b, c], Sylvain R.A. Marque [a, *]

[a] Aix Marseille Université, Institut de Chimie Radicalaire—UMR 7273, Case 551, 13397 Marseille Cedex 20, France
[b] Sartorius Stedim FMT S.A.S, Z.I. Les Paluds, Avenue de Jouques CS91051, 13781 Aubagne Cedex, France
[c] Aix Marseille Université, LISA, EA4672, Equipe METICA, 13397 Marseille Cedex 20, France

A B S T R A C T

The present work aims to investigate by ESR the effects of γ-irradiation on antioxidants and on solid multilayer films used in biomedical applications. The multilayer films analyzed here are mainly composed of polyethylene and ethylene vinyl alcohol. Radical species are monitored over time after γ-irradiation at several doses (30, 50, 115 and 270 kGy) using ESR to assess the impact of the dose-value on the formation of the radicals.

Keywords:
Electron spin resonance investigation
γ-irradiation
Polyethylene
Ethylene vinyl alcohol
Antioxidants
Additives

1. Introduction

The preparation, storage, mixing, freezing, transportation, formulation, and filling of biopharmaceutical solutions are performed in sterile single-use plastic bags. The sterilization is achieved through γ-irradiation, which generates modifications of the materials, as reported in the literature [1]. The integrity and the security of packages rely on the appropriate flexible and barrier polymeric materials such as polyethylene (**PE**) and ethylene vinyl alcohol (**EVOH**) [2]. γ-sterilization of single-use systems initiates chemical reactions inside the plastic material, leading to either an increase or a decrease in the molecular weight of the polymers [3,4]. In our work, we focused on the effects of γ-irradiation on the solid state of a multilayer **PE**/**EVOH**/**PE** polymer film, named film **A**, and on additives commonly used in this type of film [5–7]. The manufacturing of polymeric films is carried out by extruding the resin granulates. To allow the robust transformation of the resin granulates into films and to aid further manufacturing through to the finished products, additives are used to adjust the characteristics of the resin. **PE** has interesting water barrier properties and mechanical properties [8,9]. **EVOH** is remarkable for its barrier properties to CO_2 and O_2 gases [2].

The classical γ-irradiation dose range used in the biopharmaceutical industries is between 25 and 45 kGy [10]. In this study, γ-irradiation doses up to 270 kGy were investigated in order to enhance the effect of the γ-irradiation and to therefore better emphasize and investigate the modifications induced by γ-rays.

The γ-sterilization of these systems affords complex modifications inside the materials, leading to modifications of the additives or to damage in the polymers themselves [11–13]. The modifications probably induce the formation at the surface and in the core of the material of radical species that are detected by ESR (Electron Spin Resonance). The radical species are generated despite the presence of antioxidants in the films, which raises questions about the localization and the nature of these radical species. The radicals generated during the irradiation process should be quickly scavenged by the antioxidants in the layers where these additives are present [14]. The presence of oxygen-containing organic molecules results from the competition between the free-radical scavenging by antioxidants and the reaction of O_2 with the hydrocarbon chains [15]. This competition may depend on the γ-irradiation dose rate

* Corresponding author.
E-mail address: sylvain.marque@univ-amu.fr (S.R.A. Marque).

and on the direct availability of oxygen and antioxidants [15]. The generation of oxygen-containing organic molecules on the surface of the films should be higher than in their core, due to the direct contact with air, while the permeation of oxygen through the polymers is rather a slow migration process. The generation of free radicals and their diffusion in the polymers are therefore two independent phenomena resulting in different radical lifetimes, depending on which layer the radicals originate from.

The localization, nature and lifetime of the radicals generated during the γ-irradiation stage were investigated on film **A**. Film **A,** as well as some antioxidants and additives (Fig. 1) commonly used in plastic films [56-7], was investigated under different conditions: irradiated at different γ-doses under air and degassed.

2. Experimental

The films and resins investigated in this study – the three-layer film **A**, the monolayer **PE** film, the monolayer **EVOH** film and **EVOH** resins with different grades of **EVOH** – were provided by Sartorius Stedim FMT (Aubagne, France). It is worthy to note that the thickness of the **EVOH** layer is not homogeneous in the overall film. Molecules **1**–**6** were purchased from Sigma Aldrich, stored at room temperature, and used as received. Molecules **1**–**4** and **6** are generally used in manufacturing of plastic films. The internal layer is the side of film in contact with the solution when the bag is filled, and the external layer is the side of film in contact with air. Unlike in the case of a previous investigation [16], this information is not crucial as the radicals generated do not depend on the side.

Additives, films and resins were irradiated at room temperature by a ^{60}Co γ-source under air or degassed conditions. Under air, sheets of film were packed in plastic bags (made of PE) and additives or resins were introduced in glass bottles. Under vacuum, pieces of film, additive **6** or resins were all introduced in glass tubes, which were then degassed ($P = 10^{-5}$ Torr). Table 1 summarizes the mass and the conditions for each sample.

The ^{60}Co γ-source (Synergy Health company, Marseille, France) provided doses of 30 (±1), 50 (±1), 115 (±2) and 270 (±5) kGy, at a dose rate of 8–13 kGy/h. To obtain the target dose, it was necessary to perform several sterilization cycles, including a waiting time not controlled between each cycle as well as in non-controlled storage conditions.

Air irradiated samples were transferred into ESR probes (masses are reported in Table 1). The samples irradiated under vacuum conditions were quickly transferred under argon atmosphere in ESR probes, and again degassed ($P = 10^{-5}$ Torr). The additives, in pure solid form or in solution in toluene, were oxidized by PbO_2 (masses reported in Table 1).

ESR measurements were carried out on a Bruker EMX X-band spectrometer operating at 9.5 GHz and equipped with a high sensitive rectangular microwave cavity. The first spectra were recorded at room temperature a few days after γ-irradiation and the others over time.

The spectroscopic parameters were: modulation amplitude 2 G or 0.5 G (for solid and liquid additives oxidized by PbO_2, respectively), magnetic field sweep 500 G, receiver gain 10^3, resolution 1024 points, power 20.12 mW and sweep time of 20.972 s or 83.89 s (for solid and liquid additives oxidized by PbO_2, respectively). One scan was performed to record each ESR signal.

Nitroxide **7•** (see Fig. 1) was prepared according the reported procedures [18]. 45.4 mg of pure **7•** were solved in dichloromethane in order to prepare a concentration of 10^{20} molecules. The stock solution was diluted to 10^{19}, 10^{18}, 10^{17}, $5\cdot10^{16}$, $4\cdot10^{16}$, $3\cdot10^{16}$, $2\cdot10^{16}$ and 10^{16} molecules. Then 300 μL of these solutions were poured on silica gel to achieve a homogeneous powder in the ESR probe. The tubes were left open so that the dichloromethane could evaporate. Then, the ESR signals were recorded: modulation amplitude 2G, magnetic field sweep 500 G, receiver gain 10^2, resolution 1024 point, power 20.12 mW and sweeptime 20.972 s.

Masses of silica gel m, double integrals I_1 and normalized double integral I_2 are reported in Table 2. As displayed in Fig. 2, a nice correlation ($R^2 = 0.9996$) was obtained on the concentration range investigated (Table 2) affording a reliable titration curve. Nevertheless, the accuracy limit for the titration was set at $5\cdot10^{16}$ molecules and the detection threshold above 10^{16} molecules.

The calibration line is given by Equation (1), with y: the number of molecule/mg, and x: the double integral normalized with the amount of material.

$$y = -3.914\cdot10^{15} + 1.292\cdot10^{14}\cdot x \quad (1)$$

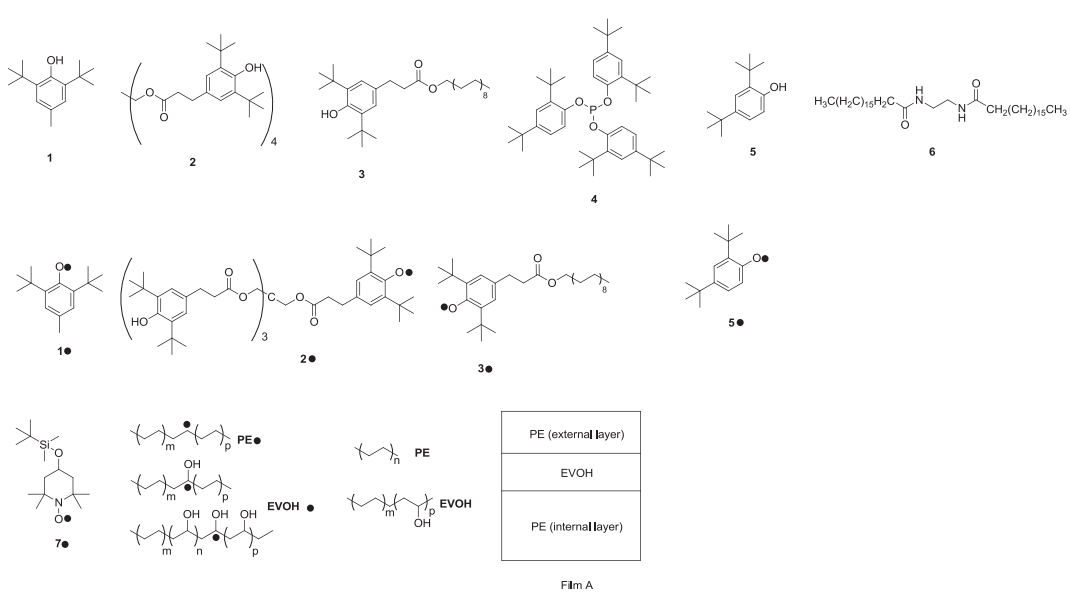

Fig. 1. Structures of additives, TEMPO derivative and film **A**. **1**: 2,6-Di-*tert*-butyl-p-cresol, **2**: Pentaerythritol tetrakis (3-(3,5-di-*tert*-butyl-4-hydroxyphenyl)propionate), **3**: Octadecyl 3-(3,5-di-*tert*-butyl-4-hydroxyphenyl)propionate, **4**: Tris (2,4-di-*tert*-butylphenyl)phosphite, **5**: 2,4-di-*tert*-butylphenol, **6**: N,N′-Ethylenebis (stearamide).

Table 1
Mass of additives, resins and films γ-irradiated (left part) or oxidized by PbO_2 (right part) introduced in the ESR tube[a].

Sample	Mass for γ-irradiation (mg)				Mass (mg)	Mass of PbO_2 (mg)
	30 kGy	50 kGy	115 kGy	270 kGy		
1	303.9	271.3	282.5	269.3	269.4	64.4
2	219.2	215.2	197.5	230.3	252.2	60.5
3	181.7	190.0	190.6	191.3	236	63.8
4	199.5	238.3	254.0	261.5	230.4	85.3
5	–	82.5	–	–	221.2	74.7
6 under air	–	197.3	–	–	162.1	60.5
6 degassed	–	150.6	–	–	–	–
Film $\mathbf{A_{50}}$ [17] under air	–	139.7	–	–	–	–
Film $\mathbf{A_{50}}$ degassed [b]	–	129.8	–	–	–	–
Film **A** under air	218.2	248.2	255.4	309.2	–	–
Film **A** degassed [b]	161.1	108.1	135.1	173.8	–	–
EVOH resin A (71% VOH) under air	–	170.5	–	–	–	–
EVOH resin A (71% VOH) degassed [b]	–	160.8	–	–	–	–
EVOH resin A (56% VOH) under air	–	194.7	–	–	–	–
EVOH resin A (56% VOH) degassed [b]	–	219.2	–	–	–	–
EVOH resin C (38% VOH) under air	–	174.9	–	–	–	–
EVOH resin C (38% VOH) degassed [b]	–	196.3	–	–	–	–
EVOH film (68% VOH) under air	–	30.9	–	–	–	–
EVOH film (68% VOH) degassed [b]	–	21.6	–	–	–	–
PE film under air	–	–[c]	–	–	–	–
PE film degassed [b]	–	84	–	–	–	–

[a] Dashed symbol – is for not investigated possibility.
[b] Degassed at $P = 10^{-5}$ Torr.
[c] ca. 100 mg.

Table 2
Number of nitroxides **7•**, double integral I_1, mass of **7•**, and normalized double integral I_2.

Number of nitroxides **7•**	I_1 (a.u. [a])	m (mg)	Number of nitroxides **7•**/m (molecules/mg)	$I_2 = I_1/m$ (a.u./mg)
10^{20}	775,000	80.1	$1.25 \cdot 10^{18}$	9675
10^{19}	91,000	79.0	$1.27 \cdot 10^{17}$	1152
10^{18}	10,000	80.0	$1.25 \cdot 10^{16}$	125
10^{17}	1300	74.4	$1.34 \cdot 10^{15}$	17
$5 \cdot 10^{16}$	800	91.8	$5.45 \cdot 10^{14}$	9
$4 \cdot 10^{16}$	600	74.5	$5.37 \cdot 10^{14}$	8
$3 \cdot 10^{16}$	800[b]	86.7	$3.46 \cdot 10^{14}$	9
$2 \cdot 10^{16}$	600[b]	71.1	$2.81 \cdot 10^{14}$	8
10^{16}	–[c]	82.0	–[c]	–[b]

[a] a.u. for arbitrary unit.
[b] Integration of traces.
[c] No signal.

All data corresponding to the quantification of ESR signals are reported in Tables SI 1-7.

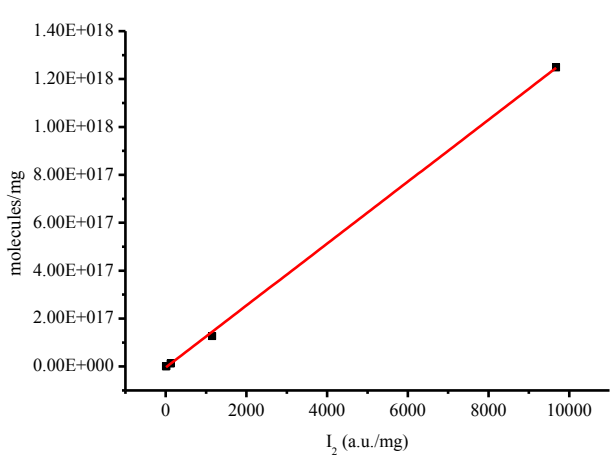

Fig. 2. Quantification limits of radicals ($R^2 = 0.9996$).

3. Results and discussion

3.1. ESR investigation of additives

Taking into account the broad linewidth ($\Delta H_{pp} \approx 4$ G) [19], the hyperfine coupling of the aromatic hydrogen atom $a_{H,m}$ ($a_{H,m} = 1.1$ G) at the *meta* position was not detected for **1•** – **3•**, and **5•** (Fig. 3a, d, g and j). Moreover, the signals expected – quadruplet for the methyl at the *para* position, triplet for the methylene at the *para* position, and doublet for the aromatic H atom at the *ortho* position – were observed for **1•** – **3•** and **5•** in toluene, with a_H values close to 10 G (Table 3). For **4•**, only traces of a species exhibiting likely an a_H value close to the one observed for **5•** are observable (Fig. 3j and m). Indeed, PbO_2 is not expected to oxidize **4** into a phosphoniumyl radical [20]. As expected, **2•** and **3•** exhibit similar signals, as **2** is roughly composed of 4 unimers of **3**. The similarities in signals for **2•** and **3•** mean that either only one phenoxy moiety was oxidized in **2•** (which we chose to display in Fig. 1 for the sake of simplicity) or no spin exchange interaction occurred between the phenoxyl moieties when several phenoxy moieties were oxidized in **2**. Thus, the ESR signals observed for the solid solution prepared by mixing PbO_2 and **1**–**3**, and **5** were

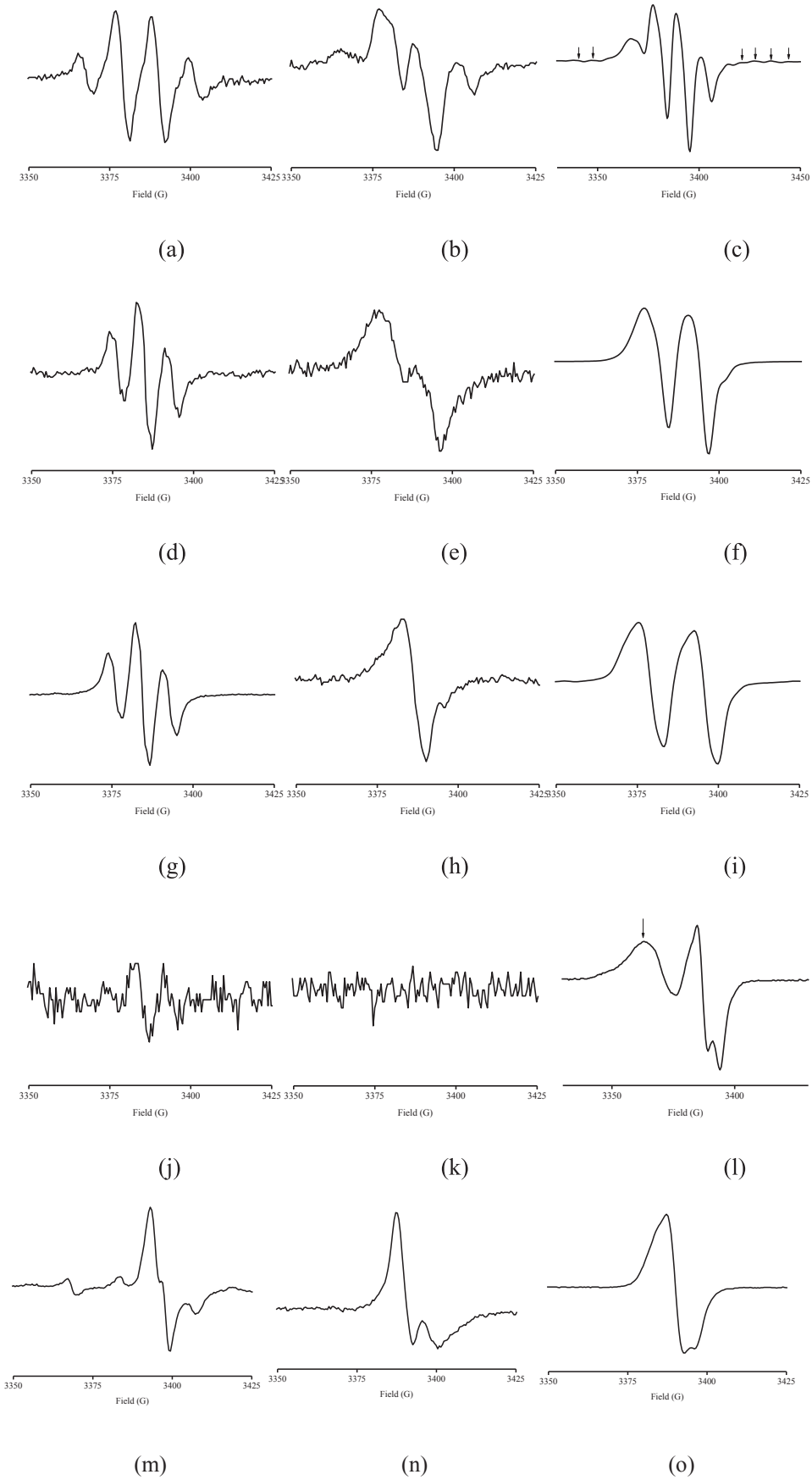

Fig. 3. ESR spectra observed after oxidation of **1**–**5** (top to bottom) recorded at RT. From left to right: oxidation by PbO_2 in toluene, oxidation in solid solution with PbO_2, and γ-irradiated at 115 kGy for c, f, i and l spectra, and at 50 kGy for o spectrum. Arrows for signals other than the signal expected for the phenoxyl radical. Signals in (a)–(c), (d)–(f), (g)–(i), (m)–(o) are ascribed to **1•**, **2•**, **3•**, and **5•**.

Table 3
Coupling constants [a] and g factors of **1•** − **3•**, and **5•** in liquid solution with PbO_2.

	1• [b]	**2•** [b]	**3•** [b]	**5•** [b]
a_{H1}	11.0	8.8	8.6	/
g	2.0047	2.0049	2.0049	2.0039

[a] In G.
[b] Structures given in Fig. 1.

ascribed to the corresponding radicals **1•** − **3•**, and **5•** (Fig. 3b, e, h and n). As expected, no signal (Fig. 3k) was observed for the solid mixture of **4** and PbO_2. The ESR signal for **1** observed after γ-irradiation is in nice agreement with the literature data. Importantly, the shape of the ESR signal was not dependent on the γ-irradiation dose for **1•**–**5•**. Interestingly, the shapes of the ESR signals corresponding to the γ-irradiated additives and to the PbO_2 oxidized additives in solid phase are very close, confirming the identical nature of the radical observed, e.g., the phenoxyl radical **1•** of additive **1**. The splitting between the major lines corresponds to the a_H values in toluene. γ-irradiation of **2** and **3** affords the same ESR doublet signal exhibiting broad lines. Although less obvious than for **1•**, γ-irradiated ESR signals for **2•** and **3•** are similar to the signals observed for the PbO_2 oxidized powder. Indeed, for this powder, an asymmetrical single line can be observed in place of the expected doublet. The better resolution for the γ-irradiated sample is likely due to the depletion of oxygen under the experimental conditions [21]. For **5•**, the unsymmetrical structure affords a signal exhibiting an anisotropy which is similar to that of the EPR signal observed for the PbO_2 oxidized powder. In sharp contrast to the results obtained for **4** either in liquid or powder form with PbO_2 as oxidant, a clear ESR signal was recorded for powder **4** after γ-irradiation. The non-symmetric signal observed for **4** after γ-irradiation, is due to the presence of two species: one species, corresponding to **5•** (very similar signal, right part of signal in Fig. 3l, see overlay in Fig. 1 SI, and $g = 2.0044$ for the right hand side of the signal), and an unknown species (left broad line in Fig. 3l, see overlay in Fig. 1 SI). Nevertheless, no phosphorus centered radicals were detected [22], meaning they were either not generated (unlikely) or too unstable to be detected (more likely). Moreover, the amount of degraded product was too small to be detected by ^{31}P NMR.

The Landé factors g for **1•** − **3•**, and **5•** in toluene are around 2.0048, as expected for phenoxyl radicals ($g = 2.0045$) [23,24]. Assuming a weak anisotropy of signals for the PbO_2 oxidized powder as well as for the γ-irradiated powder, the g-factors were straightforwardly determined and reported as 2.0048, 2.0043, 2.0044 and 2.0042, 2.0044, and 2.0046, respectively, confirming that the radical is a phenoxyl type radical. The spectra for irradiated additive **6•** under air and degassed are displayed in Fig. 4. The

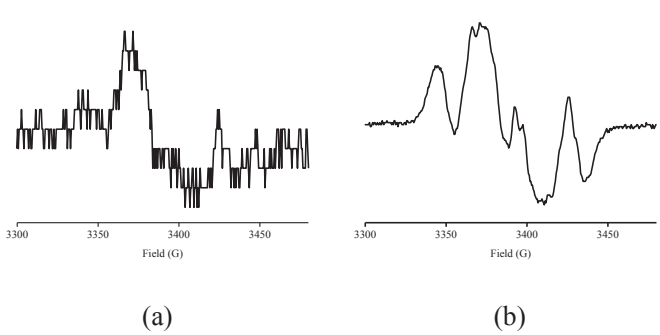

Fig. 4. ESR spectra for **6** recorded at RT and γ-irradiated at 50 kGy under air (a) and degassed (b).

strong anisotropy of the signal for **6•** hampers its simple analysis. Nevertheless, the same signal is observed under air and vacuum conditions although the signal observed under air is weaker [25]. No ESR signal is detected for molecule **6** in solid or liquid solution with PbO_2, as expected (not shown).

At this time, **6•** has not been identified. However, its kinetic behavior denotes the presence of a radical highly reactive to O_2, which is expected from alkyl, aminyl or aminiumyl radicals. As far as we know, the time evolution of γ-irradiated additives has only been reported for additive **1**. The time evolutions at room temperature of irradiated additive radicals **1•** to **4•** and **6•** are reported in Fig. 5 (Fig. 3SI) and Fig. 6 (Fig. 4SI). Concerning Fig. 5, it can be seen that radicals **1•** to **4•** are rather stable over time. The ESR signals are at least 3 orders of magnitude above the limit of detection and quantification. Radical **6•** (Fig. 6a) is highly unstable under air and disappears totally after two weeks, in sharp contrast to radicals **1•**–**4•**, whereas **6•** is stable over time in the thoroughly degassed sample (Fig. 6b). A 3-fold increase in concentration for irradiation at 30 and 50 kGy was observed during the first two months after irradiation, as reported in the literature [26]. ESR signals of samples irradiated at 115 and 270 kGy were always recorded on the same day, so the sharp decrease in signal that can be observed at 6 and 8 weeks is likely due to an experimental problem. Moreover, the intensity of this signal rises back to the level it reached before the 6th week.

3.2. γ-irradiation of *PE* film

Under air as well as under vacuum, no ESR signals were detected in **PE** upon γ-irradiation, whatever the doses received (Fig. 7a and b respectively). Obviously, the generated radicals are not stable in air at room temperature and in degassed conditions ($P = 10^{-5}$ Torr), even though they are trapped in a matrix.

3.3. γ-irradiation of *EVOH* film and resins

Whatever the conditions (under air or vacuum), the ESR signals (Fig. 8d and h) recorded on a film exhibit a nice 1:4:1 triplet, as reported [27–30] and ascribed to the **EVOH•** species (Fig. 1). However, the wings of this triplet are very weak when recorded for three types of resin (Fig. 8a–c, e–g). This difference is ascribed to the shape of the materials, that is, the polymer chains in resins [31] are likely folded and randomly oriented whereas in films the polymer chains are expected to be unfolded and oriented [32]. The hyperfine coupling of 30.4 G observed for the 1:4:1 triplet of film is very close to the 32 G reported by Rao et al. [27].

The g-factors are listed in Table 4 and are all around an average value of 2.0038, which is in the expected range for hydroxyl alkyl radicals ($g = 2.0030$) [33–38].

Whatever the conditions (air or vacuum), the **EVOH•** generated by γ-irradiation at 50 kGy are stable for at least 3 months (Fig. 9 and Fig. 5SI).

Interestingly, γ-irradiation of **EVOH** under air did not generate radical species stable enough to be detected by ESR, except **EVOH•** (Fig. 9). Moreover, the same amount of radicals was generated under air and in vacuum conditions. Furthermore, **EVOH•**, which is a C-centered radical, was as stable under air as it was in vacuum (Fig. 9).

These results nicely highlight the O_2-barrier properties of **EVOH** materials.

3.4. γ-irradiation of film *A*

Film **A** was investigated after two sterilization campaigns. For the first campaign, film **A** was irradiated at 30, 50, 115 and 270 kGy,

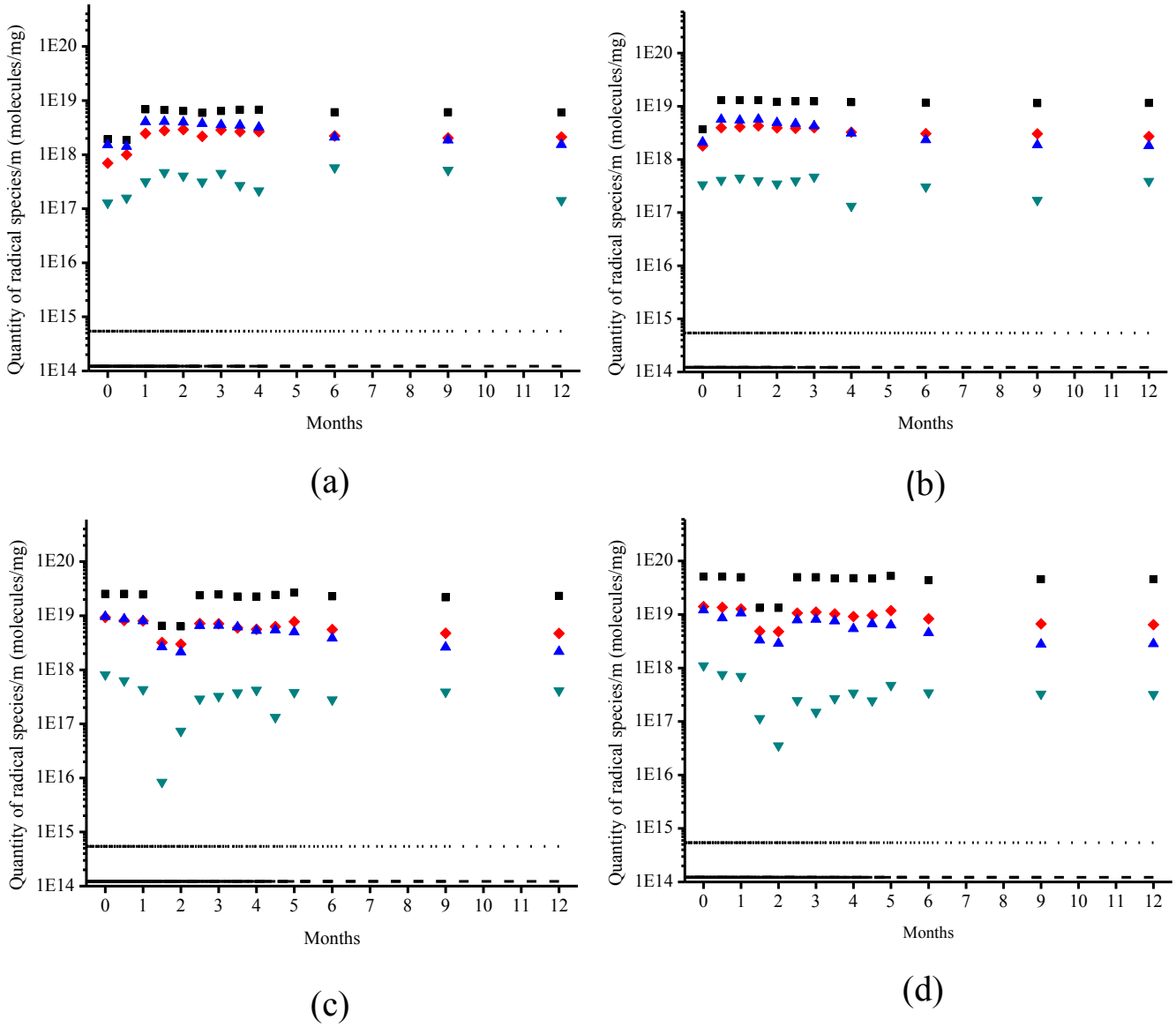

Fig. 5. Time evolution of 1 ■, 2 ◆, 3 ▲, 4 ▼ at RT in semi-log scale for various doses: (a) 30 kGy, (b) 50 kGy, (c) 115 kGy, (d) 270 kGy. Dotted line for quantification limit at $5.5 \cdot 10^{14}$ molecules/mg, dashed line for detection limit at $1.2 \cdot 10^{14}$ molecules/mg.

and for the second one, at 50 kGy (Film $\mathbf{A_{50}}$).

3.4.1. Under vacuum

In order to compare our results to literature results, and to be in the absence of O_2, samples were degassed under high vacuum ($P = 10^{-5}$ Torr). It should be mentioned that the vacuum measurement values found in the literature are around 1 mTorr [28].

The ESR signal observed for film $\mathbf{A_{50}}$ as well as film **A** at other doses is strikingly different from those observed for **EVOH** resins and film, i.e., no wings and splitting of the central line. This ESR signal is not due to the **PE** layers (no ESR signal for **PE**, vide supra). It is likely that the ESR signal for **6•** superimposed upon the signal for **EVOH•**. This signal disappears under O_2 bleaching (vide infra). Interestingly, the signal changes during the first month, the extra coupling almost disappears (Fig. 10c). After a 42% signal loss in 2 weeks, the amount of radicals remained constant over 11 weeks (Fig. 10b and Fig. 6SI). The second radical likely generated by γ-irradiation of **6** was less stable under vacuum, in contrast to Fig. 6b, probably because of the presence of several additives in the **EVOH** layer. When γ-irradiation was performed at 30, 50, 115 and 270 kGy on film **A**, the results were similar to those obtained for 50 kGy, whatever the dose.

Low variations in the amount of radicals with time and sharp signal changes are observed (Figs. 10c and 11b) meaning that the other species was generated in small amount but exhibited a strong signal. This agrees with the assumption of a species being generated by γ-irradiation of **6**.

3.4.2. Under air

Films **A** and $\mathbf{A_{50}}$ exhibit ESR signals (1:4:1) (Fig. 12a and Fig. 13b, respectively) similar to those reported for **EVOH** film and resins. Film **A** is a 3 layer PE/EVOH/PE material containing various types of additives able to provide ESR signals. The *g* factor was roughly estimated as $g_{iso} = 2.0036$, in nice agreement with the *g* factor reported for **EVOH** resins and film (Table 4). The wing line/central line ratio is constant over time, pointing that the wing and central lines belong to the same species. As observed with **EVOH** resins and film, the ESR signal for film $\mathbf{A_{50}}$ was stable for 13 weeks (Fig. 12b

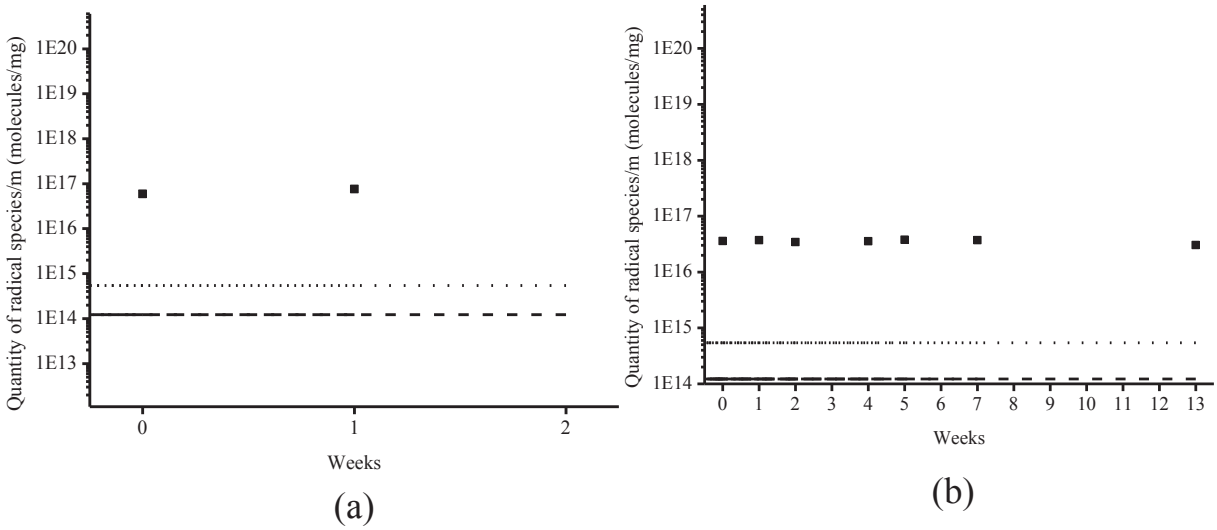

Fig. 6. Time evolution of **6•** at RT in semi-log scale for a dose of 50 kGy: (a) under air, (b) degassed. Dotted line for quantification limit at $5.5 \cdot 10^{14}$ molecules/mg, dashed line for detection limit at $1.2 \cdot 10^{14}$ molecules/mg.

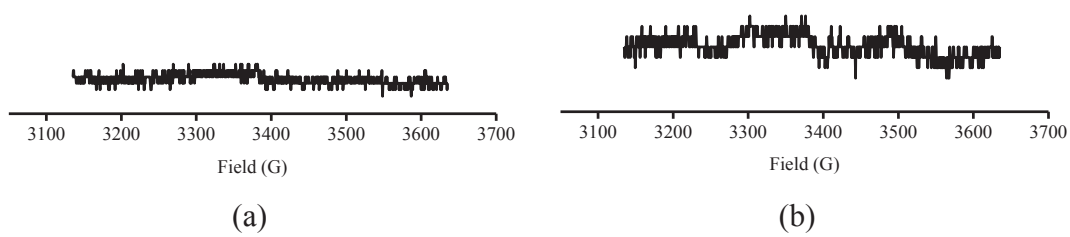

Fig. 7. ESR spectrum of contact layer (**PE**) irradiated at 50 kGy (a) under air, (b) degassed at RT.

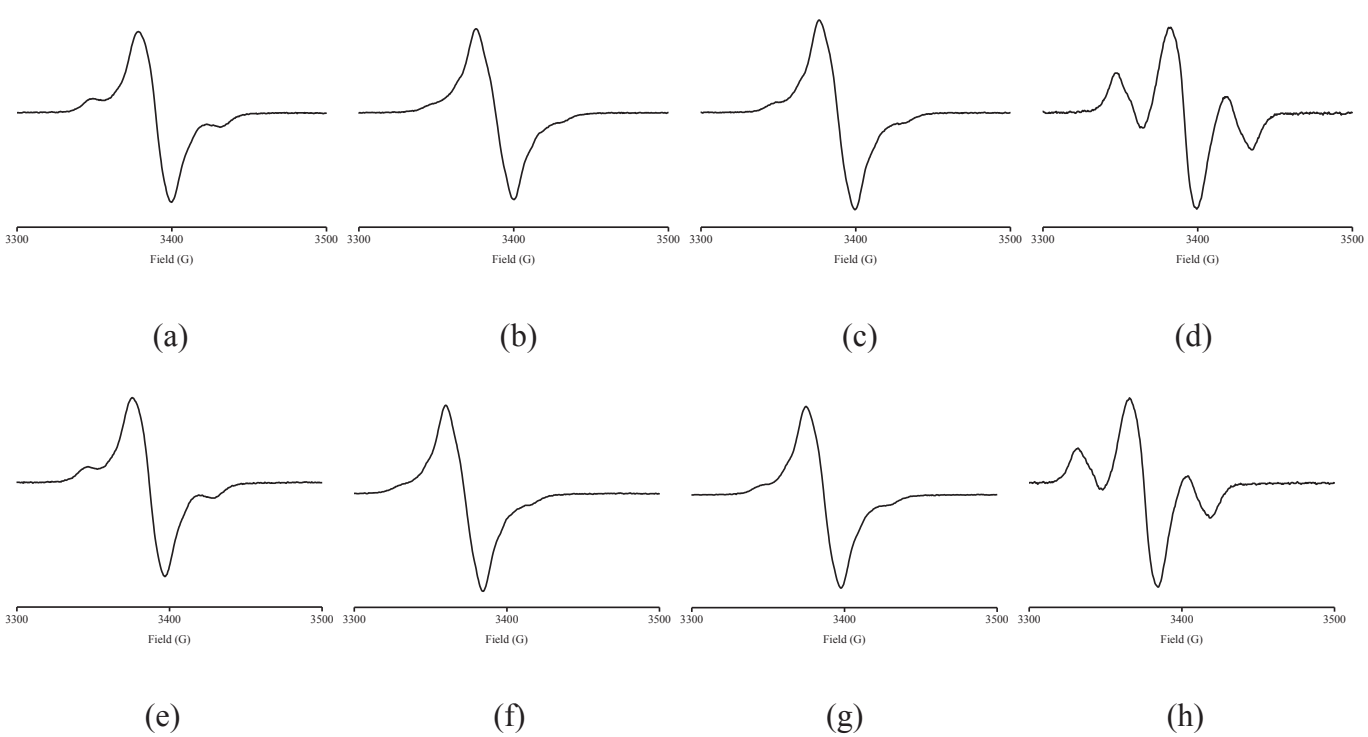

Fig. 8. ESR spectra for **EVOH** resins and film irradiated at 50 kGy and at RT under air: (a) resin A, (b) resin B, (c) resin C, (d) film; and under vacuum: (e) resin A, (f) resin B, (g) resin C, (h) film.

Table 4
g-factors for **EVOH** resins and film irradiated at 50 kGy under air and degassed.

Landé factor	Resin A		Resin B		Resin C		Film	
	Under air	Degassed	Under air	Degassed	Under air	Degassed	Under air	Degassed
g_x	2.02853	2.02811	2.02911	2.02805	2.02891	2.02763	2.02947	2.02965
g_y	2.00367	2.00382	2.00423	2.00424	2.00432	2.00421	2.00344	2.00349
g_z	1.97941	1.97925	1.97938	1.97928	1.97976	1.97936	1.97778	1.97772
g_{iso} [a]	2.0039	2.0037	2.0042	2.0039	2.0043	2.0037	2.0036	2.0036

[a] $g_{iso} = (g_x + g_y + g_z)/3$.

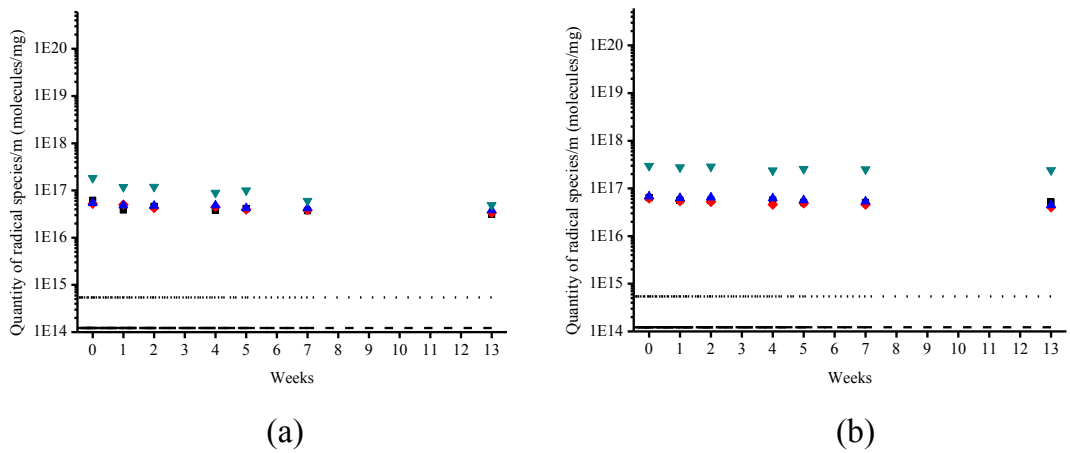

Fig. 9. Quantity of radical species in **EVOH** resins and film over time (in week) in semi-log scale (a) under air (b) under vacuum (resin A ■, resin B ◆, resin C ▲, film ▼) at RT. Dotted line for quantification limit at $5.5 \cdot 10^{14}$ molecules/mg, dashed line for detection limit at $1.2 \cdot 10^{14}$ molecules/mg.

and Fig. 8SI). Accordingly, the ESR signal observed for film **A** is ascribed to radical R–CH_2-C•(OH)–CH_2-R from **EVOH**. On the other hand, film **A,** when irradiated at either 50, 115 or 270 kGy, displays an ESR signal up to 1 month, whereas when irradiated at 30 kGy, it displays a signal up to 10 weeks. Moreover, more radicals are observed in film **A** (10^{17}–10^{18} molecules/mg) than in film $\mathbf{A_{50}}$ (10^{16} molecules/mg). This discrepancy between the two series of irradiation is likely due to both the experimental conditions of irradiation, leading to a difference in concentration, and the heterogeneity of film **A**, i.e., the thickness of the **EVOH** layers varying by several micrometers. Nevertheless, the same qualitative comments hold for both series.

4. Conclusion

It is clear that γ-irradiation affords hydroxyalkyl radicals in

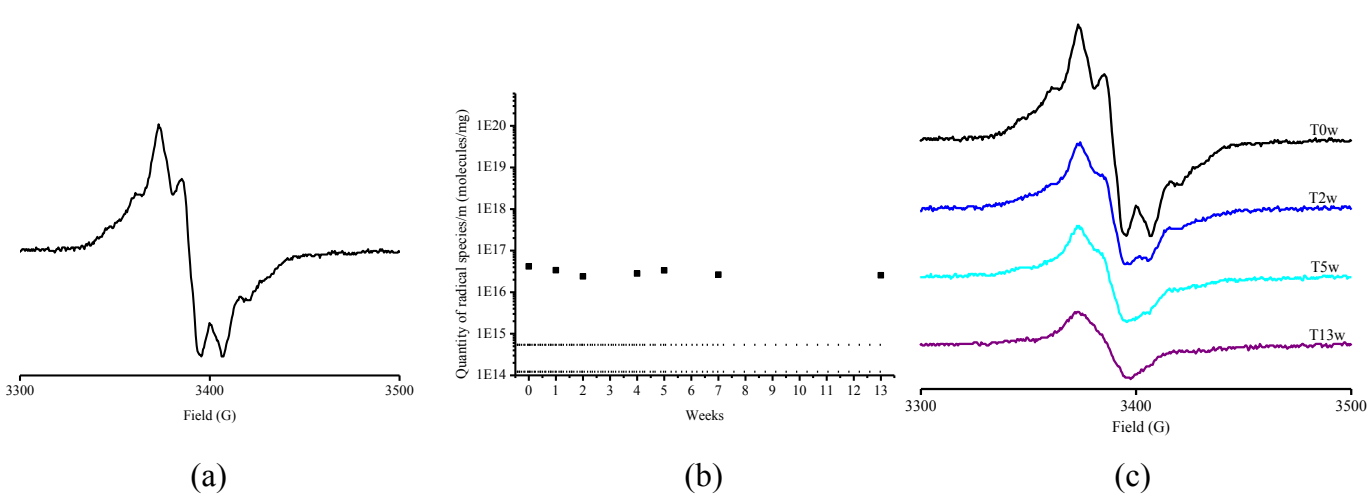

Fig. 10. Film $\mathbf{A_{50}}$ (degassed) irradiated at 50 kGy: (a) ESR spectrum, (b) quantity of radical species over time in semi-log scale. Dotted line for quantification limit at $5.5 \cdot 10^{14}$ molecules/mg, dashed line for detection limit at $1.2 \cdot 10^{14}$ molecules. (c) ESR spectra of over time.

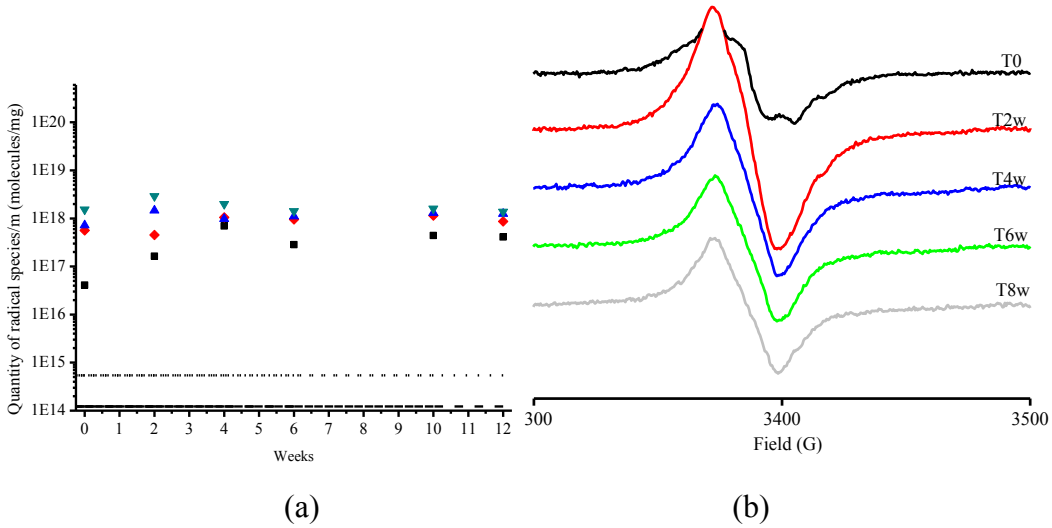

Fig. 11. (a) Quantity of radical species in film **A** (degassed) over time in semi-log scale at different doses: 30 kGy ■, 50 kGy ◆, 115 kGy ▲, 270 kGy ▼. Dotted line for quantification limit at $5.5 \cdot 10^{14}$ molecules/mg, dashed line for detection limit at $1.2 \cdot 10^{14}$ molecules. (b) ESR spectra of film **A** (degassed) irradiated at 270 kGy over time.

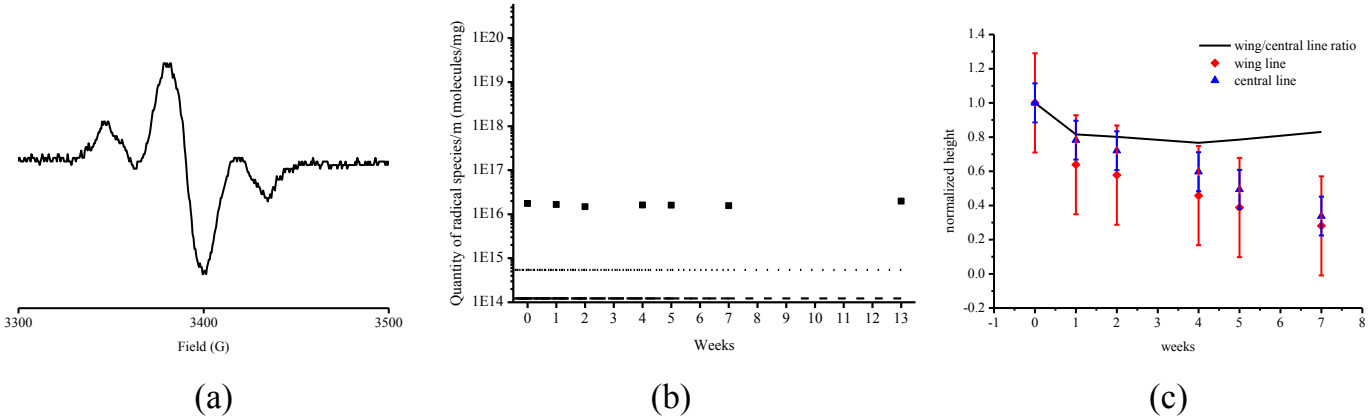

Fig. 12. Film $\mathbf{A_{50}}$ (under air): (a) ESR spectrum, (b) quantity of radical species over time. Dotted line for quantification limit at $5.5 \cdot 10^{14}$ molecules/mg, dashed line for detection limit at $1.2 \cdot 10^{14}$ molecules. (c) Wing line decay over time ◆, central line decay over time ▲, solid line corresponds to wing/central line ratio.

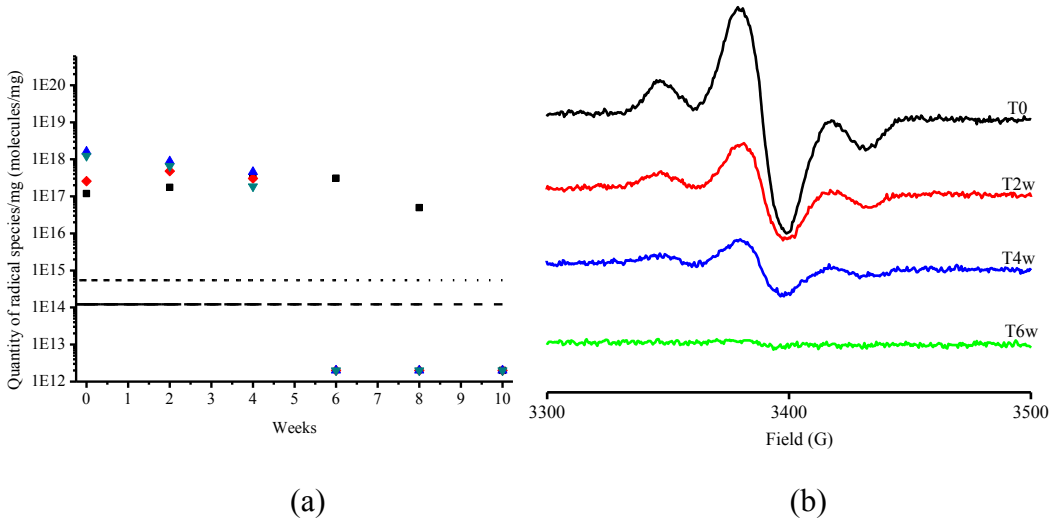

Fig. 13. (a) Quantity of radical species of film **A** (under air) over time (30 kGy ■, 50 kGy ◆, 115 kGy ▲, 270 kGy ▼). Dotted line for quantification limit at $5.5 \cdot 10^{14}$ molecules/mg, dashed line for detection limit at $1.2 \cdot 10^{14}$ molecules. (b) ESR spectra for film **A** irradiated at 270 kGy over time.

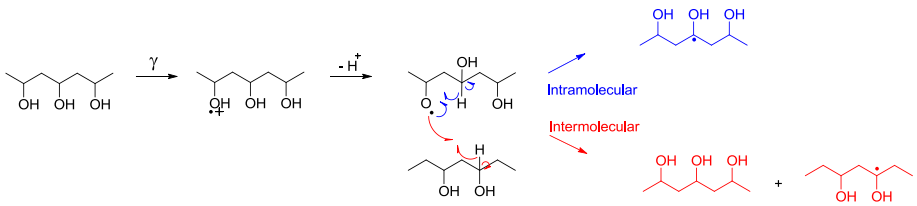

Scheme 1. Different radical pathways to generate hydroxyalkyl radical-type.

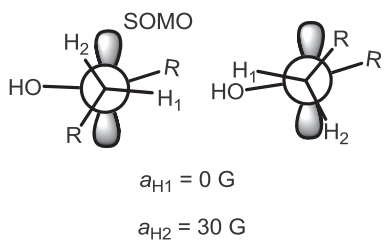

Scheme 2.

EVOH, whatever the doses and the experimental conditions. Hydroxyalkyl radicals are probably 3rd generation radicals from the primary oxoniumyl radical, as depicted in Scheme 1. Indeed, the oxoniumyl radical spontaneously releases a proton to generate an oxyl radical, which in turn generates a hydroxyalkyl radical by H-abstraction either from another chain or through an intramolecular process (1,4-H-transfer). The 1:4:1 pattern requires a conformation with an H atom either eclipsed or anti to the •C—OH bond (Scheme 2).The stability of **EVOH•** to O_2-bleaching confirms the low permeability of the **EVOH** layer to O_2.

Acknowledgments

FG thank Sartorius Stedim Biotech for PhD grant. ND and SRAM are thankful to AMU and CNRS for support, and to Sartorius Stedim Biotech for funding.

Appendix A. Supplementary data

Supplementary data related to this article can be found at http://dx.doi.org/10.1016/j.polymdegradstab.2015.10.021.

References

[1] A. Traboulsi, N. Dupuy, C. Rebufa, M. Sergent, Investigation of gamma radiation effect on the anion exchange resin Amberlite IRA-400 in hydroxide form by Fourier transformed infrared and ^{13}C nuclear magnetic resonance spectroscopies, Anal. Chim. Acta 717 (2012) 110–121.
[2] A.E. Goulas, K.A. Riganakos, M.G. Kontominas, Effect of ionizing radiation on physicochemical and mechanical properties of commercial multilayer coextruded flexible plastics packaging materials, Radiat. Phys. Chem. 68 (2003) 865–872.
[3] M. Driffield, E. Bradley, L. Castle, Literature Review, Analytical Screening and Chemical Migration Studies on Irradiated Food Packaging, 2009.
[4] J.C.M. Suarez, E.B. Mano, Characterization of degradation on gamma-irradiated recycled polyethylene blends by scanning electron microscopy, Polym. Degrad. Stabil. 72 (2001) 217–221.
[5] D.H. Jeon, G.Y. Park, I.S. Kwak, K.H. Lee, H.J. Park, Antioxidants and their migration into food simulants on irradiated LLDPE film, LWT 40 (2007) 151–156.
[6] F. Bourges, G. Bureau, J. Dumonceau, B. Pascat, Effects of electron beam irradiation on antioxidants in commercial polyolefins: determination and quantification of products formed, Packag. Technol. Sci. 5 (1992) 205–209.
[7] J. Pospisil, Chemical and photochemical behaviour of phenolic antioxidants in polymer stabilization-a state of the art report, Part I, Polym. Degrad. Stabil. 40 (1993) 217–232.
[8] Tirtha Chatterjee, Rajen Patel, John Garnett, Rajesh Paradkar, Shouren Ge, Lizhi Liu, Kenneth T. Forziati Jr., Nik Shah, Machine direction orientation of high density polyethylene (HDPE): barrier and optical properties, Polymer 55 (2014) 4102–4115.
[9] M. Tolinski, Additives for Polyolefins, second ed., 2015, pp. 171–173.
[10] Guide to Irradiation and Sterilization Validation of Single-use Bioprocess Systems, BioProcess International, may 2008 supplement, 10–22.
[11] K.J. Hemmerich, Medical device and diagnostic industry, online, http://www.mddionline.com/article/polymer-materials-selection-radiation-sterilized-products, 2000.
[12] N.H. Stoffers, J.P.H. Linssen, R. Franz, F. Welle, Migration and sensory evaluation of irradiated polymers, Radiat. Phys. Chem. 71 (2004) 203–206.
[13] P.G. Demertzis, R. Franz, F. Welle, The effects of γ-irradiation on compositional changes in plastic packaging films, Packag. Technol. Sci. 12 (1999) 119–130.
[14] R. Gensler, C.J.G. Plummer, H.-H. Kausch, E. Kramer, J.-R. Pauquet, H. Zweifel, Thermo-oxidative degradation of isotactic polypropylene at high temperatures: phenolic antioxidants versus HAS, Polym. Degrad. Stabil. 67 (2000) 195–208.
[15] Y. Ohkatsu, T. Matsuura, M. Yamato, A phenolic antioxidant trapping both alkyl and peroxy radicals, Polym. Degrad. Stabil. 81 (2003) 151–156.
[16] F. Gaston, N. Dupuy, S.R.A. Marque, S. Dorey, Chemometric methods coupled with Raman spectroscopy applied to assessing the impact of gamma irradiation on multilayer films, submitted in Anal, Chim. Acta (2015).
[17] Film A50 is the film A irradiated at 50kGy. Another Steriliz. campaign was performed 30, 50, 115 and 270 kGy doses.
[18] C.D. Anderson, K.J. Shea, S.D. Rychnovsky, Strategies for the generation of molecularly imprinted polymeric nitroxide catalysts, Org. Lett. 22 (7) (2005) 4879–4882.
[19] Solutions of toluene were not degassed.
[20] If such oxidation would have been occurred, the generated phosphoniumyl radial is not expected to be stable enough to be detected and the degradation processes are expected to afford in detectable amounts **5•**.
[21] The γ-irradiation of materials is likely to generate alkyl radicals or hydrogen atoms which are prone to react quickly with O2 leading to a depletion of its interaction and then less spin-spin interactions with the phenoxyl radical affording narrower lines.
[22] Whatever the type of centered phosphorus radicals – phosphinyl, phosphonyl, phosphoranyl, and phosphoniumyl – a large phosphorus hyperfine coupling constant should have been detected S. Marque, P. Tordo, Landolt-bornstein Magnetic Properties of Radicals, Phosphorus-centered Radicals, Radicals Centered on Other Heteroatoms, Group. 2, in: Organic Radical Ions, vol. 26, 2008. Subvolume E, 7 – 81.
[23] For $C_{15}H_{23}O•$ in Landolt-Börnstein II/9c2, 79.
[24] R.D. Parnell, K.E. Russel, An electron spin resonance study of the second-order decay of 4-alkyl-2,6-di-t-butylphenoxyl radicals in solution, J. Chem. Soc. Perkin Trans. II (1974) 161–164.
[25] To compare the effect of irradiation, signal under air was recorded with the same acquisition parameters than the signal degassed. Due to the very low concentration of radicals, the signal has a very poor signal/noise ratio (Fig. 4a).
[26] H. Tuner, M. Korkmaz, Radiostability of butylated hydroxytoluene (BHT): an ESR study, Nucl. Instrum. Meth. B 258 (2007) 388–394.
[27] B.S. Rao, M. Ramakrishna Murthy, Electron spin resonance and UV absorption of irradiated poly(vinyl alcohol), J. Polym. Sci. Pol. Phys. 25 (1987) 1897–1902. Experimental conditions: Poly(vinyl alcohol) powder irradiated in air at RT.
[28] B.H. Milosavljevic, J.K. Thomas, Radiation induced processes in the copolymer, polyethylene-poly(vinyl alcohol), Nucl. Instrum. Meth. B 208 (2003) 185–190. Experimental conditions: copolymer PE-co-PVA film irradiated in vacuum (1 mTorr) at 77K up to 298 K.
[29] Zainuddin, David J.T. Hill, Tri T. Le, An ESR study on γ-irradiated poly(vinyl alcohol), Radiat. Phys. Chem. 62 (2001) 283–291. Experimental conditions: Poly(vinyl alcohol) powder irradiated in vacuum (10-2 Pa) at 77K.
[30] P.K. Wong, Nature of trapped free radicals in γ-irradiated poly(vinyl alcohol) films, Polymer 19 (1978) 785–788. Experimental conditions: Poly(vinyl alcohol) film irradiated in vacuum (10-4 Torr) at RT.
[31] The ESR signal do not depend on the amount of EVOH in materials (Table 1).
[32] For their experiments, Rao et al. used powder of EVOH and ^{60}Co source at 4 kGy/h.
[33] For $CH_3CH_2CH_2C•(OH)CH_2CH_2CH_3$ in Landolt-Börnstein II/9b, 193, 217–218.
[34] G.B. Birrell, O.H Griffith, Electron spin resonance study of x-irradiated long-chain alcohols oriented in urea inclusion crystals, J. Phys. Chem. 75 (1971) 3489–3491.
[35] F.P. Sargent, Electron spin resonance studies of radiation damage. Part I. An alternating linewidth effect for the $(CH_3)_2C•OH$ radical in gamma-irradiated

acetone at low temperatures, Can. J. Chem. 46 (1968) 1029–1031.
[36] A.P. Kuleshov, V.I. Trofimov, Radical formed during γ-irradiation of alkyl halides in urea, High. Energy Chem. 6 (1972) 82–83.
[37] D. Greatorex, T.J. Kemp, Electron spin resonance studies of photo-oxidation by metal ions in rigid media at low temperatures, Trans. Faraday Soc. 67 (1971) 56–66.
[38] H. Paul, H. Fisher, Elektronenspinresonanz freier Radikale bei photochemischen Reaktionen von Ketonen in Lösung, Helv. Chim. Acta 56 (1973) 1575–1594.